PERMANENT DEFORMATION, STIFFNESS DEGRADATION AND STRENGTH OF OPEN HOLE GLASS/PA6 UD THERMOPLASTIC COMPOSITE IN TENSION AND COMPRESSION

Ruben, Sevenois[a], Wim Van Paepegem[a]

a: Department of Materials, Textiles and Chemical Engineering, Faculty of Engineering and Architecture, Ghent University, Technologiepark Zwijnaarde 46, B-9052 Zwijnaarde, Belgium

Abstract: *The permanent deformation, stiffness degradation and strength of UD Glass/PA6 coupons with an open hole under tension and compression loading is investigated. 3 layups: $[0/90]_{5s}$ and $[+45/-45]_{5s}$ and $[+45/0/-45/90]_{3s}$ were tested. The specimen shape was rectangular with a width of 36 mm and a hole size of 6 mm, according to ASTM D5766. Both monotonic loading as well as Loading-Unloading-Reloading tests were executed. This, together with a measure of the full field strain of the sample (using Digital Image Correlation) allowed to identify the general sample strength as well as identify several regions where permanent deformation and damage occurred.*

Keywords: open hole; thermoplastic; Experimental; Digital Image Correlation

1. Introduction

While for Thermoset Fibre Reinforced Polymers (TS FRP) [1–3] detailed studies about the failure behaviour in the presence of stress concentrations exist, they seem to be absent for Thermoplastic Fibre Reinforced Polymers (TP FRP). Also, there is an increasing interest for advanced material models which are able to predict the nonlinear behaviour of TP-FRP. For an in-depth validation of such material models detailed information is required about the strain field evolution during the loading process. In addition, knowledge of the quantitative evolution of specimen stiffness and permanent strain, which may be caused by a combination of damage phenomena including matrix cracking and plastic deformation, fiber failure, fiber-matrix debonding and delaminations is crucial input for such numerical models.

In this work UD Glass/PA6 laminates with an open hole are subjected to tension (OHT) and compression (OHC) loading. Both monotonic and Loading-Unloading-Reloading (LUR) tests were executed to identify the evolution of specimen stiffness and the development of permanent strain on the specimen surface.

2. Methodology

Laminated plates were hot pressed with TenCate CETEX UD glass/nylon-6 from Ten Cate Advanced Composites B.V. Laminated plates with layup $[0/90]_{5s}$ and $[+45/-45]_{5s}$ were produced from which rectangular specimens were cut using water jet cutting. Afterwards a central hole with diameter 6 mm, to avoid damage to the hole edges, was milled from the composite coupons. *Figure **1*** shows the specimen dimensions. The specimens with 250 mm length were used for tensile tests. The specimens with 150 mm length were used for compressive tests. A summary of the test program is given in *Table **1***.

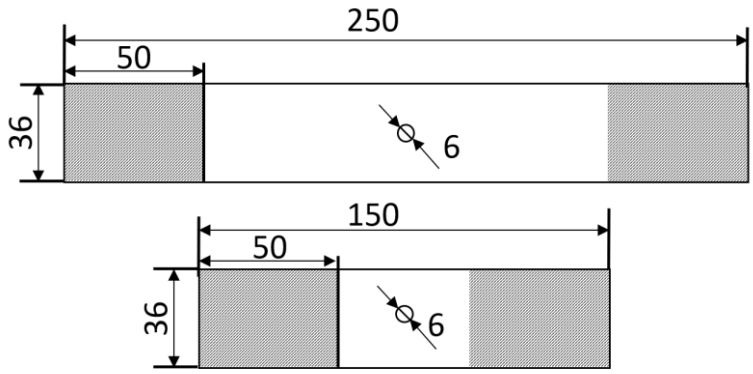

Figure 1: Specimen shapes. Top: tensile specimen. Bottom: compression specimen. The grey area is the clamped area

The specimens were tested on a 100 kN hydraulic Instron uniaxial test bench. The clamps of the machine were aligned before testing to ensure proper load introduction. The specimens were inserted over the full clamp length. Thus, the effective gauge length was 150 mm and 50 mm for, respectively, the tensile and compressive specimens. Both monotonic loading until failure as well as Loading Unloading Reloading (LUR) tests were executed. In the LUR tests consecutive reloadings were done at approximately 25%, 35%, 50%, 65% and 85% of the static strength after which the specimen was loaded until fracture.

The strain on the sample surface was measured using 3D Digital Image Correlation (DIC). For this the specimen surface was first painted with white, water based, acrylic airbrush paint. This type of paint adheres well to the surface while it does not form a film. The latter ensures that, when large deformations occur, the paint does not detaches or peels from the specimen surface. The 3D DIC system consisted of a custom setup with 2 Pointgrey cameras with 5MP resolution. The images were calibrated and analysed using the software VIC-3D from Correlated Solutions.

Table 1: Overview of specimens and load type

Load type	Layup	Length [mm]	Width [mm]	Thickness [mm]	Hole diameter [mm]	Actuator. Speed [mm/min.]
Monotonic tensile LUR Tensile	$[0/90]_{5S}$	250	36	5.2	6	2
	$[+45/-45]_{5S}$	250	36	5.2	6	2
	$[+45/0/-45/90]_{3s}$	250	36	6.2	6	2
Monotonic compression LUR Compression	$[0/90]_{5S}$	150	36	5.2	6	0.5-0.6
	$[+45/-45]_{5S}$	150	36	5.2	6	0.5-0.6
	$[+45/0/-45/90]_{3s}$	150	36	6.2	6	0.5-0.6

From the testdata several aspects such as the observed failure phenomena, the general stress-strain behaviour, the development of permanent strain and apparent damage (sample stiffness reduction) is investigated. For the global specimen stress-strain behaviour, the nominal stress,

$\sigma_{nom.}$, is calculated by dividing the force from the load cell with the initial cross sectional area at the maximum hole width as shown in Equation 1.

$$\sigma_{nom} = \frac{F}{(w-d)*t}$$

Equation 1

In Equation 1, F is the force from the load cell, w is the sample width, t is the sample thickness and d is the hole diameter. The global sample strain is defined as the engineering strain between two points located close to the clamps, as indicated in *Figure 2*. Due to the presence of the hole, the authors stress that the forthcoming stress-strain curves of these experiments indicate specimen behaviour and not intrinsic material behaviour.

An example of the global stress-strain behaviour for a LUR-OHT test with layup $[+45/-45]_{5s}$ is shown in Figure 2. One can clearly see the development of permanent strain after each loading cycle. Furthermore, the specimen stiffness is defined as the slope between consecutive maximum and minimum loads in an unloading-reloading cycle. This is indicated by the straight black lines.

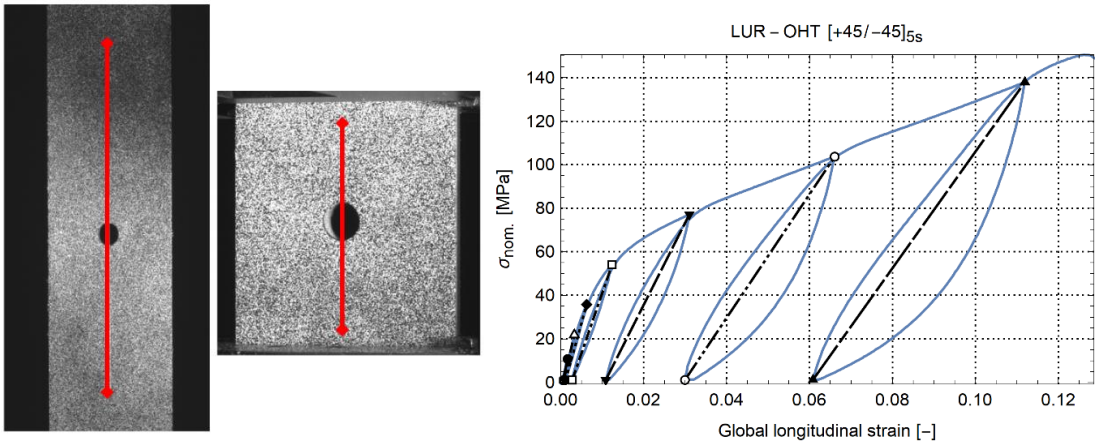

Figure 2: Global sample strain gauge for tension (left) and compression (right) specimen, b) Nominal stress- global strain of an open hole sample with layup $[+45/-45]_{5s}$ under tension load.

3. Results and Discussion

In this section the global specimen stress-strain behaviour is discussed in Section 3.1. Then, in Section 3.2 the observed failure type for each type is discussed. This is followed by a discussion about the development of permanent strain and damage in Section 3.3.

3.1 Nominal stress – global strain

The nominal stress - global strain of the experiments is shown in Figure 3. The result for each layup is represented by a different colour. For the results of samples with the same layup, different dashing is used.

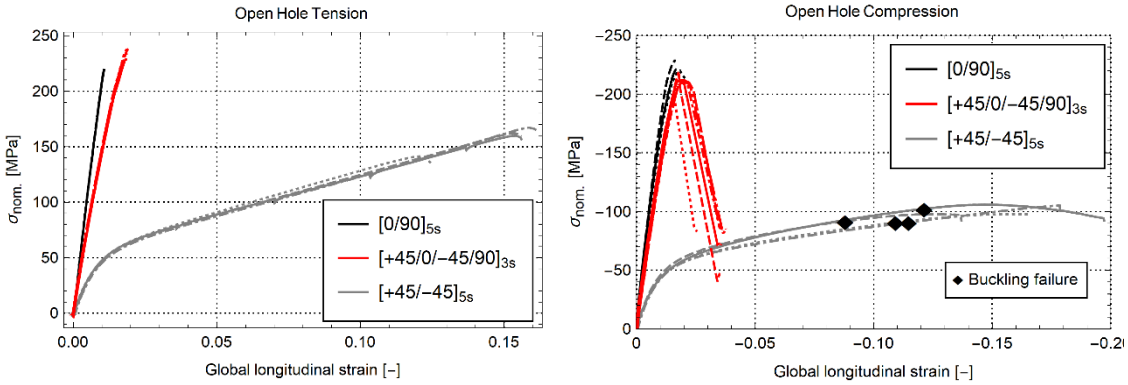

(a) (b)

Figure 3: Nominal stress vs global strain of samples subjected to monotonic loading until failure. a) OHT, b) OHC

The cases for OHT are shown in Figure 3a. The coupons with layup $[0/90]_{5s}$ and $[+45/0/-45/90]_{3s}$ show quasi-linear behaviour up to sudden failure at about 220 MPa. The coupon with layup $[+45/-45]_{5s}$ initially shows linear behaviour and becomes nonlinear at 1% strain. A failure strain of about 12-15% is observed with a failure load of about 150 MPa. These failure strains are significantly higher than for the other specimens because the +45/-45 plies are primarily loaded in shear, which illustrates the large deformation capability of the PA6 matrix. Remarkable is that the OHT strength of the QI laminate is higher than the OHT strength of the coupon with layup $[0/90]_{5s}$. This is caused by the high OHT strength of the +45/-45 plies in the QI laminate.

The data for OHC are shown in Figure 3b. Similar to tension, layups $[0/90]_{5s}$ and $[+45/0/-45/90]_{3s}$ show quasi-linear behaviour up to failure. A small non-linear region is present close to final failure. After kinking at maximum load the QI samples were still able to carry about 35% of the maximum strength at -75 MPa. The curves for layup $[+45/-45]_{5s}$ are non-linear. A notable difference is that buckling occurs at about -90 MPa, as indicated by the black diamonds. The end of the curves for $[+45/0\text{-}45/90]_{3s}$ and $[+45/-45]_{5s}$ do not indicate specimen failure. The specimens were removed after, respectively, kinking and buckling to protect the load cell of the machine and preserve the crosshead alignment. Yet, the specimens could still have been compressed further.

3.2 Failure observations

For each of the six combinations of load (tensile and compressive) and layup ($[0/90]_{5s}$ and $[+45/-45]_{5s}$, $[+45/0/-45/90]_{3s}$) different failure phenomena were observed.

Figure 4 shows images of typical failure behaviour of the samples with layup $[0/90]_{5s}$ under, respectively, tensile and compressive load. OHT failure of the samples with layup $[0/90]_{5s}$ shows no indication of growing cracks up till sudden failure. Despite the sudden breakage large symmetrical cracks appear from the sides of the holes and span almost the entire width of the sample. At the sides of the specimen a number of fibers are still bridging over the crack, effectively holding both specimen halves together. Although this connection is weak, it indicates that next to fibre breakage also fibre pull-out is an important damage phenomenon. OHC failure of the samples with layup $[0/90]_{5s}$ show relatively sudden kinking failure. Just before failure initial localized kinking can be observed originating from the hole edge. This is very difficult to

see visually, however, they can be spotted with the DIC strain field through a local strain concentration, or local correlation failure of the strain field.

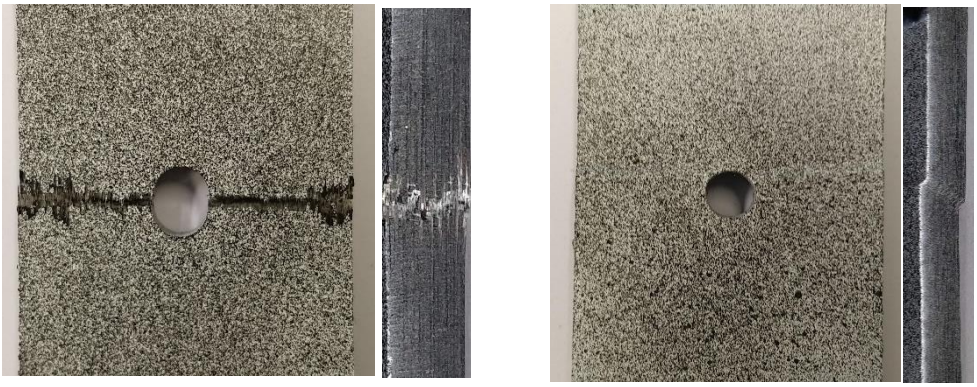

a) b)

Figure 4: Front and side view of ultimate failure of Glass/PA6 laminate, layup $[0/90]_{5s}$, with 6 mm diameter hole in a) tension, b) compression

For the samples with layup $[+45/-45]_{5s}$ both tensile and compressive loading showed large non-linear behaviour before failure. Figure 5 shows typical observations under, respectively, tensile and compressive loading. OHT failure for layup $[+45/-45]_{5s}$, Figure 5a, shows a combination of crack growth and ductile failure. Before failure multiple cracks develop at the hole edge. However, note that not all cracks necessarily grow to cause final failure. In Figure **5**a, a crack is indicated with a red circle. Although this crack appears to be the largest before failure, the crack causing load bearing failure occurs from a different location. OHC failure for layup $[+45/-45]_{5s}$, Figure **5**b **Error! Reference source not found.**, could not be achieved. The samples showed very high nonlinear deformation before eventually buckling at about 90-100 MPa σ_{nom}, Figure 3b. This shows the very high sample deformation which could be observed. After the occurrence of buckling, samples were unloaded and removed.

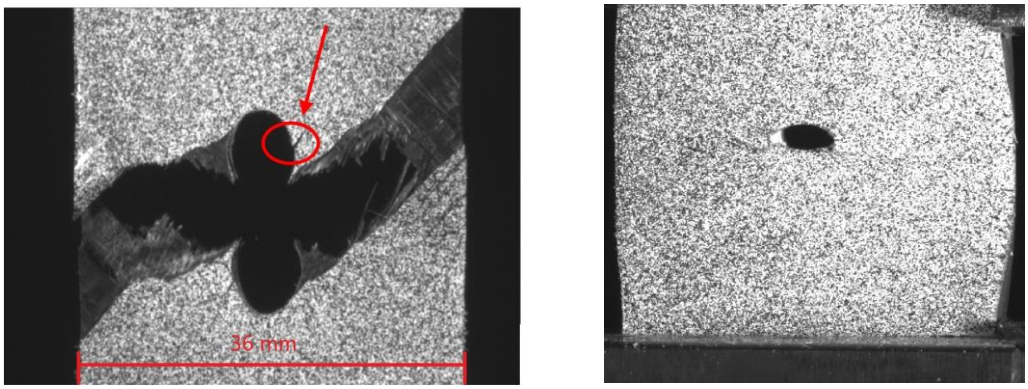

(**a**) (**b**)

Figure 5: Failure for laminate $[+45/-45]_{5s}$ a) tensile, b) compressive

Figure 6 shows the tensile and compressive failure for specimen with layup $[+45/0/-45/90]_{3s}$. For the tensile case, cracks develop along the +45 fibre direction of the top ply. These grow from the hole edge towards the edges of the sample until final failure. The specimen fails in a brittle way due to the presence of the 0 degree plies. The [0] plies show fibre pull-out with delamination, [90] plies show matrix cracking and the [45] plies failed in the typical shear-out

failure. Similar to $[0/90]_{5s}$; the compressive failure of $[+45/0/-45/90]_{3s}$ occurs in the form of kinking, Figure 6b. Buckling was not observed during loading. It is noted, however, that the specimens do not fracture in two pieces as seen from the side view. The delamination damage is contained within the kinking zone. The combination of plies in all three primary directions is able to keep the plies from both sides of the specimen connected and attached, even after severe kink deformation. This allows the specimen to carry load after initial failure.

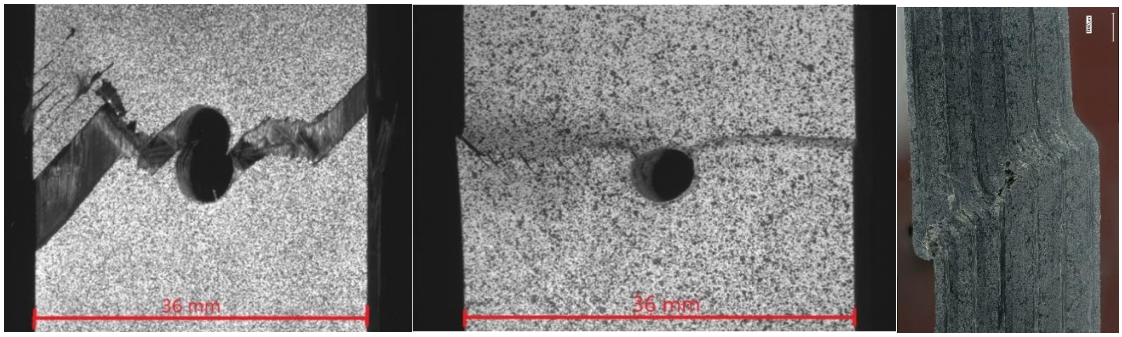

a) b)

Figure 6: Failure for laminate $[+45/0/-45/90]_{3s}$ a) tensile, b) compressive + side view

3.3 Stiffness and permanent strain evolution

Figure 7 shows the evolution of permanent strain and modulus of the specimen with layup $[+45/-45]_{5s}$. In the figures, the same symbols are used for the same test. The datapoints in gray occurred after buckling. A large amount of permanent strain occurs, and the elastic modulus reduces with each load cycle up to about 30% of the original modulus for tension, and 40% (before buckling) for compression. Between tensile and compression loading the evolution of permanent strain is similar, the evolution of specimen elastic modulus is less steep for compression.

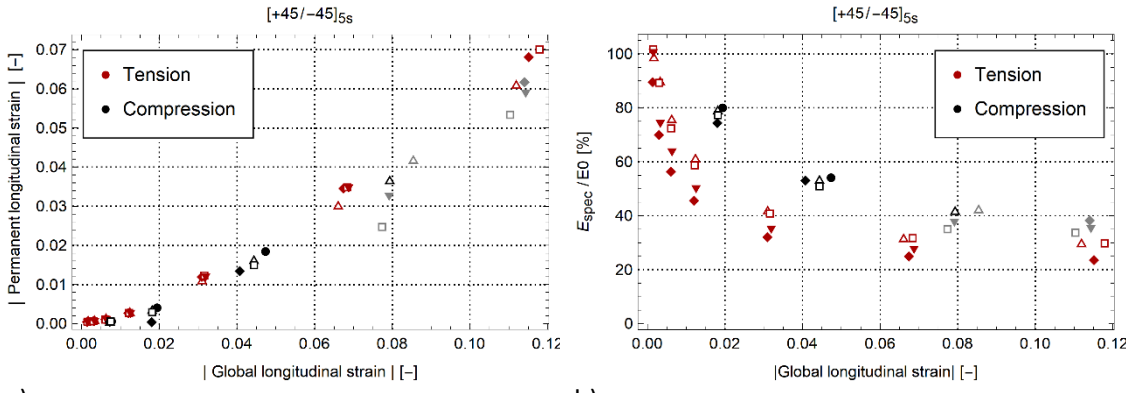

a) b)

Figure 7: a) Permanent strain and b) evolution of normalized elastic modulus for $[+45/-45]_{5s}$. Datapoints in gray are measured after buckling.

Figure 8 shows the evolution of longitudinal permanent strain and elastic modulus for $[0/90]_{5s}$ and $[+45/0/-45/90]_{3s}$. Though the nominal stress- global strain curve is quasi-linear, both layups show a small evolution in global permanent strain with a modulus reduction of about 20%. This suggests that, at least locally, some damage and plasticity occurs in the specimen volume. Similar evolutions are shown between tension, compression, and per layup. Note the initially

higher elastic modulus after the first unloading cycle in the compression data of Figure 8b. This is caused by variability in strain measurement at small strain magnitude. Despite this, both elastic modulus evolution and permanent strain evolution are similar for tension and compression.

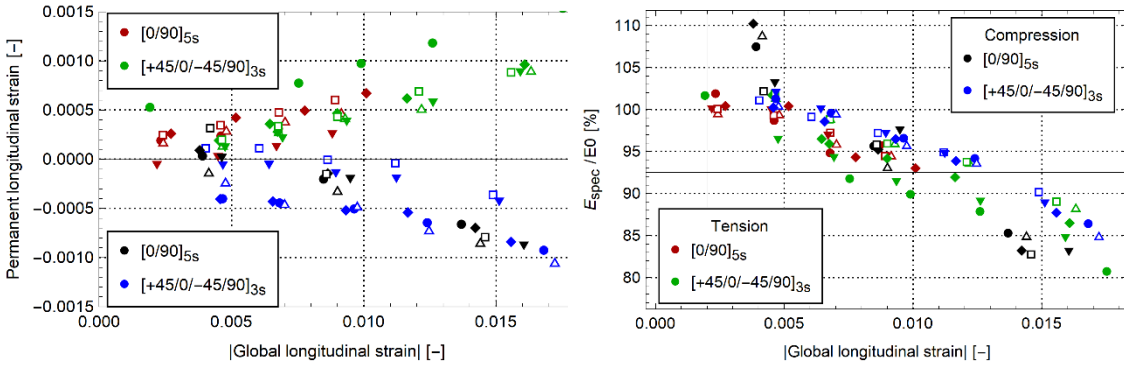

a) b)

Figure 8: a) Permanent strain and b) normalized elastic modulus for $[0/90]_{5s}$ and $[+45/0/-45/90]_{3s}$.

Figure 9 shows the longitudinal strain on the specimen surface for the layup $[+45/-45]_{5s}$ and $[0/90]_{5s}$ at unloading after either the last load cycle or just before buckling. For the samples with layup $[+45/-45]_{5s}$ X-shaped shear bands with high permanent strain develop. These meet at the side of the hole. This is illustrated in Figure 9a for the tensile case where the longitudinal strain is positive. For compression the longitudinal strain has the same shape, yet with negative sign. For the samples with layup $[0/90]_{5s}$, Figure 9b, a region of nearly zero longitudinal strain occurs above and below the hole center. To the left and right of the hole a local region with permanent strain occurs. For the compressive case the pattern is similar. The region with larger permanent strain is limited to the immediate vicinity of the hole. The permanent strain pattern for the QI layup shows a combination of the patterns from the $[0/90]_{5s}$ and $[+45/-45]_{5s}$ laminates.

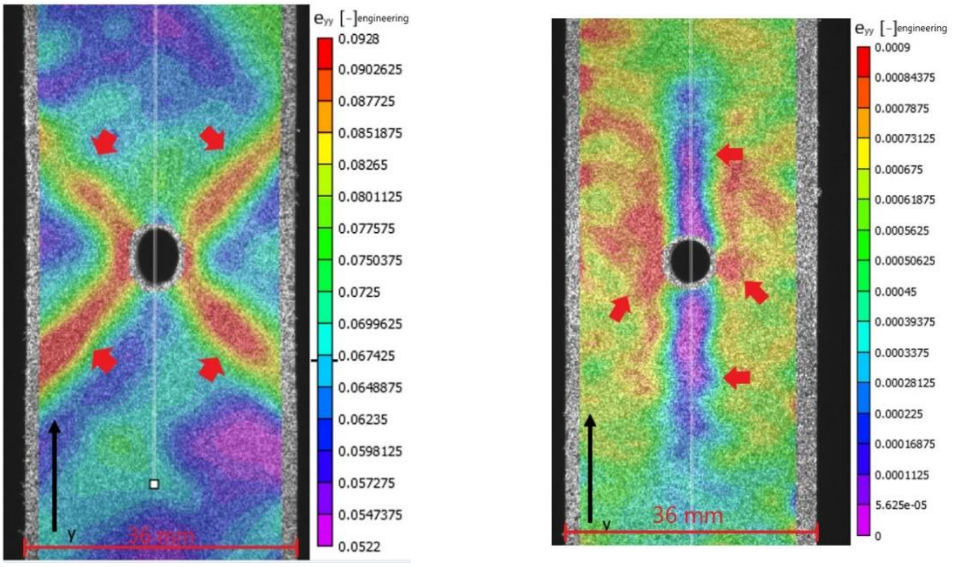

a) b)

Figure 9: Permanent strain developed after unloading specimen a) LUR-OHT with layup $[+45/-45]_{5s}$ and b) $[0/90]_{5s}$after the highest loading cycle before failure

4. Conclusion

In this work Open Hole Tension and Open Hole Compression tests were executed on three laminates from UD Glass/PA6 material. The laminates tested are $[0/90]_{5s}$, $[+45/-45]_{5s}$ and $[+45/0/-45/90]_{3s}$. Both monotonic and Loading-Unloading-Reloading experiments were executed. This allowed to identify global specimen behaviour, the development of permanent strain, and evolution of specimen elastic modulus until final failure.

The experimental results show the significant nonlinear behaviour of Open Hole specimens made from thermoplastic fibre reinforced materials under both tensile and compressive loading. The specimens with layup $[+45/-45]_{5s}$ showed similar behaviour under both tension and compression. A degradation of the specimen elastic modulus up to 70% and permanent longitudinal strain of 7% is seen. The specimens with layup $[0/90]_{5s}$ and $[+45/0/-45/90]_{3s}$ show a maximum reduction of about 20% in elastic modulus. A very small amount of 0.1 % permanent longitudinal strain is noted.

The availability of the entire strain field on the sample surface throughout the test can be used to verify and validate finite element simulations of open hole tests for this material. A remarkable observation is that, while the evolution of global permanent strain and elastic modulus reduction between the tensile and compressive load cases is quite similar, the distribution of permanent strain development can be different. This indicates the necessity to include full field strain measurements, as well as both tensile as compressive loading, in future experimental programs on composite mechanical behaviour.

Acknowledgements

This research was funded by Research Foundation Flanders FWO, grant number 12R3221N.

References

[1] Clay SB, Knoth PM. Experimental results of quasi-static testing for calibration and validation of composite progressive damage analysis methods. J Compos Mater 2016;0:1–21. https://doi.org/10.1177/0021998316670132.

[2] Hinton M, Kaddour a. Triaxial test results for fibre-reinforced composites: The Second World-Wide Failure Exercise benchmark data. J Compos Mater 2012. https://doi.org/10.1177/0021998312459782.

[3] Kaddour AS, Hinton MJ, Smith PA, Li S. Mechanical properties and details of composite laminates for the test cases used in the third world-wide failure exercise. J Compos Mater 2013;47:2427–42. https://doi.org/10.1177/0021998313499477.

